RSC Advance

Electronic Supplementary Information

Selective fluorometric detection of F^- and Zn(II) ions by *N*, *O* coordinating sensor and naked eye detection of Cu(II) ion in mixed-aqueous solution †

Amar Hens and Kajal Krishna Rajak*

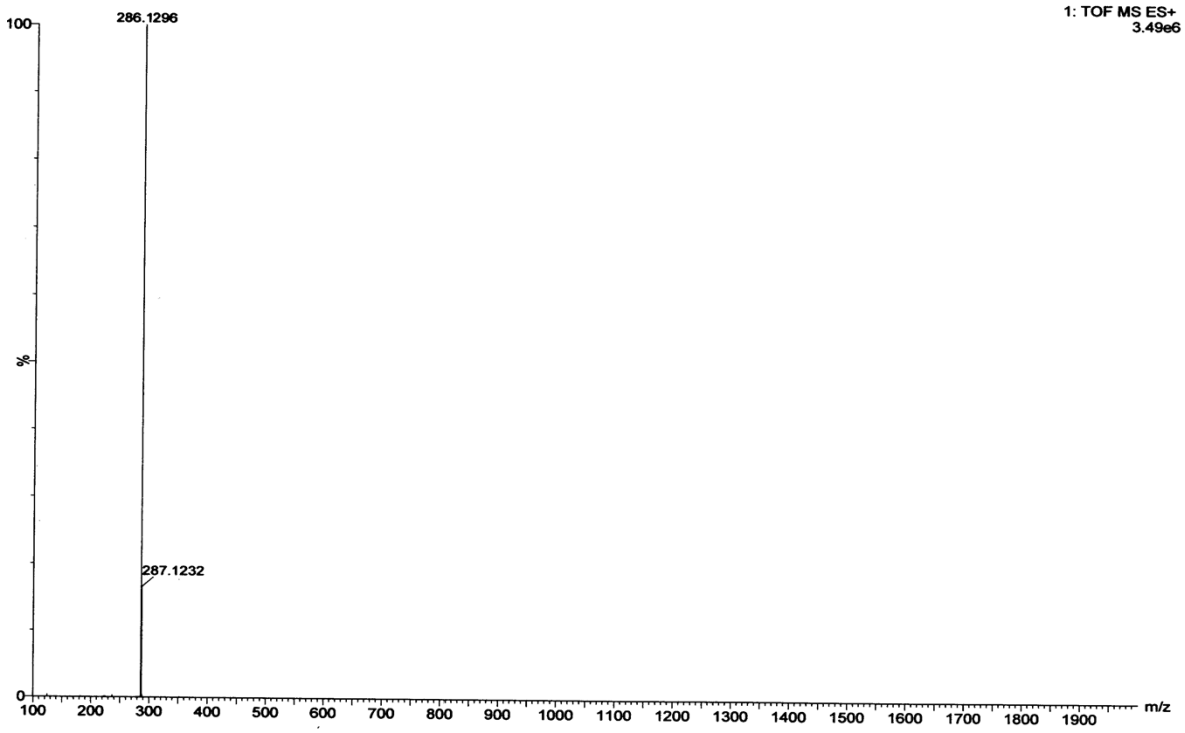

Fig. S1 High-resolution mass spectrum of a solution containing HL in acetonitrile.

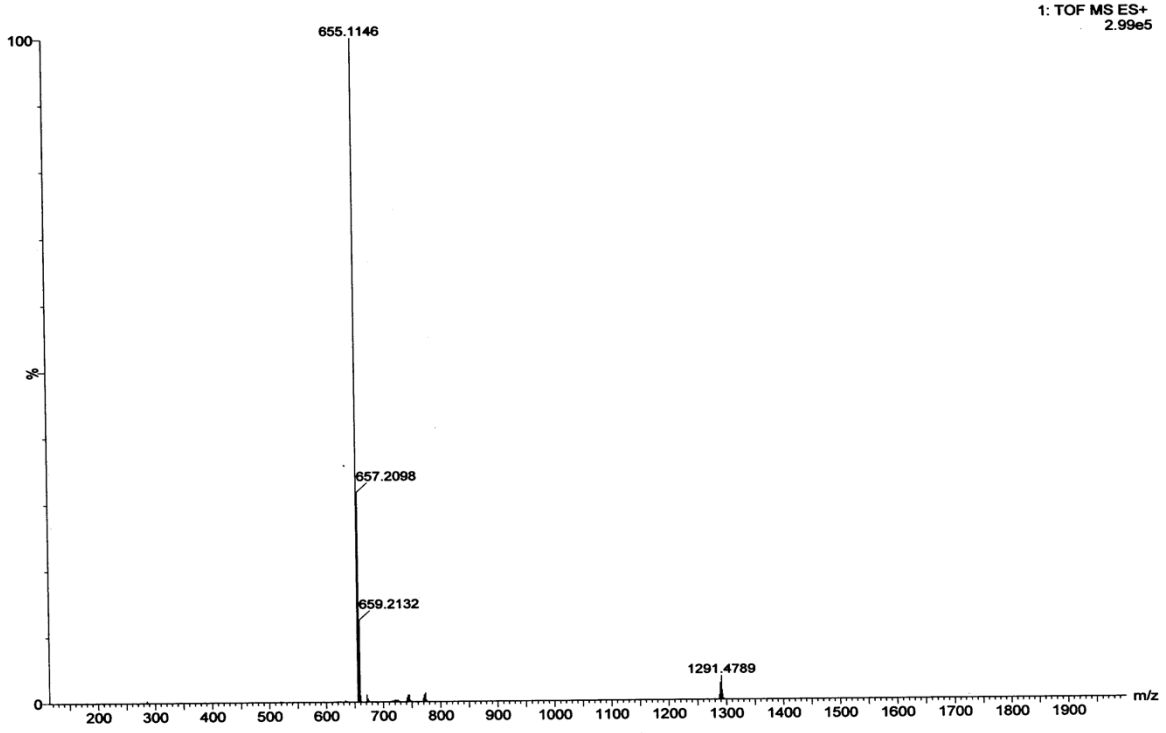

Fig. S2 High-resolution mass spectrum of a solution containing $Zn(L)_2$ in acetonitrile.

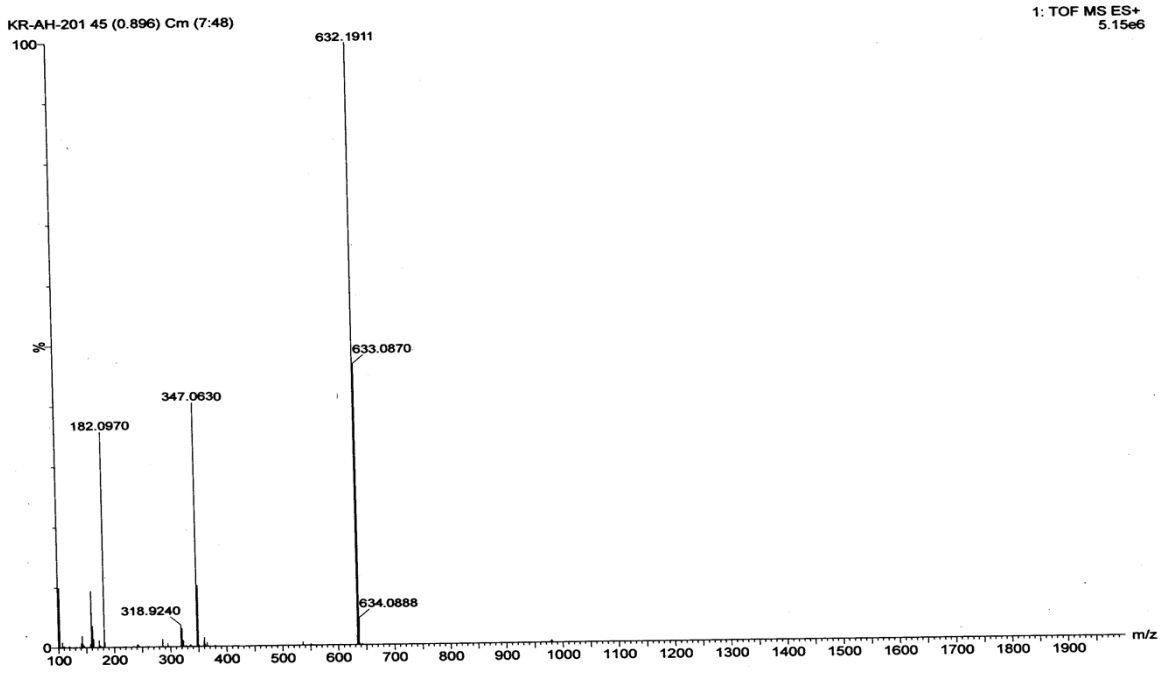

Fig. S3 High-resolution mass spectrum of a solution containing $Cu(L)_2$ in acetonitrile.

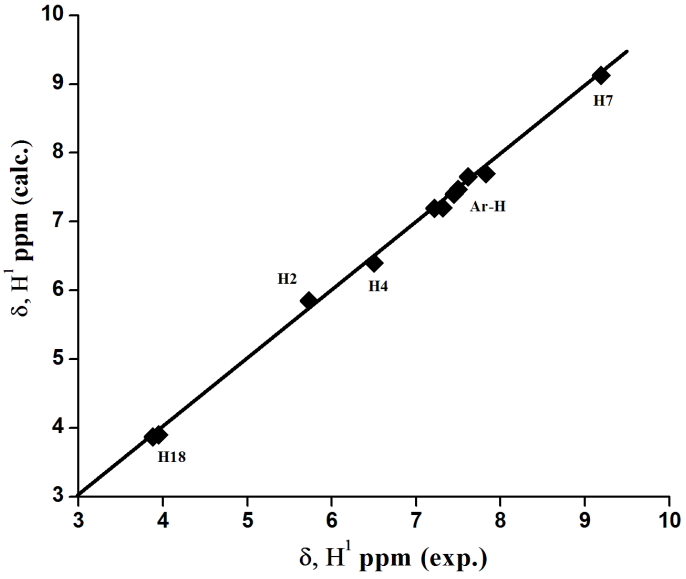

Fig. S4. Linear correlation between the experimental and calculated ^{1}H NMR chemical shifts of **1** in aliphatic and aromatic regions.

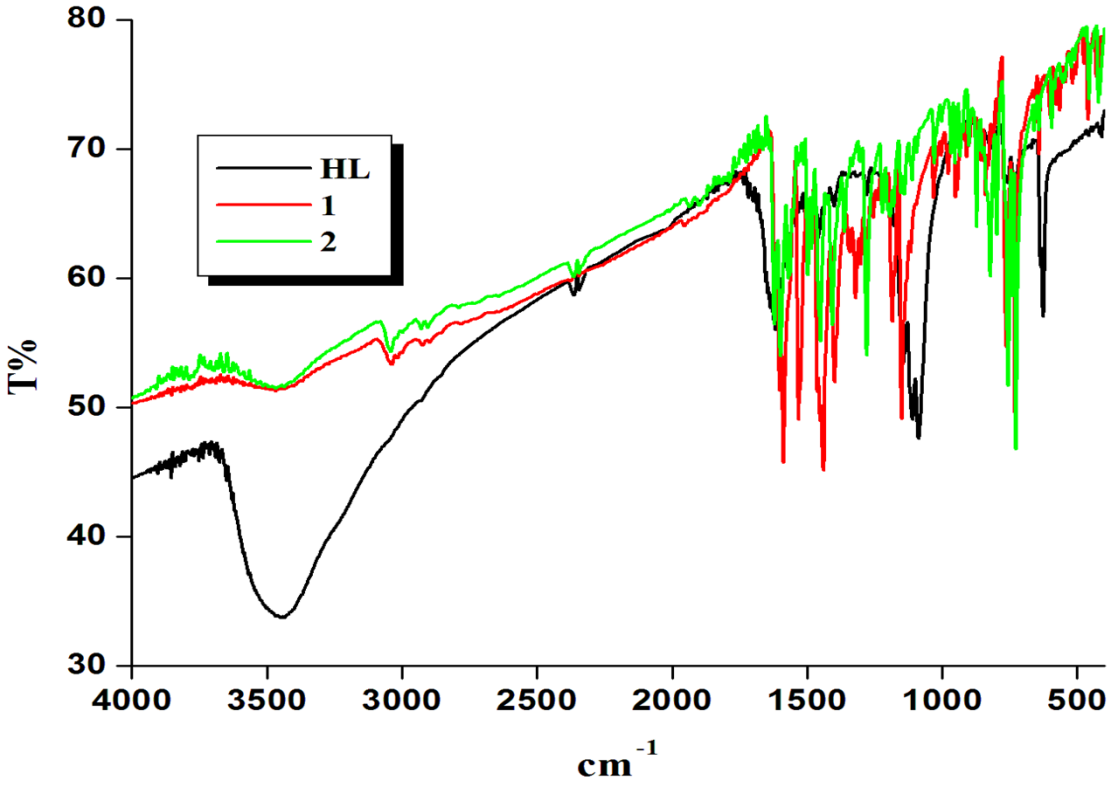

Fig. S5 IR spectrum of HL and complexes at room temperature.

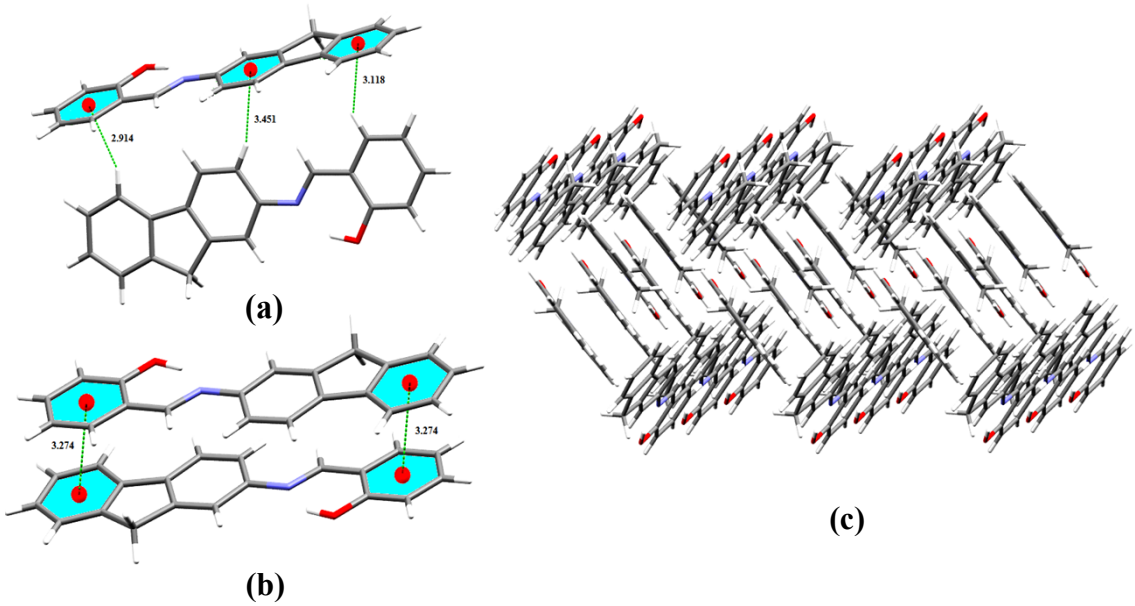

Fig. S6 Several C-H/π interactions (a) π…π interactions (b) and 2D extended pattern (c) of HL.

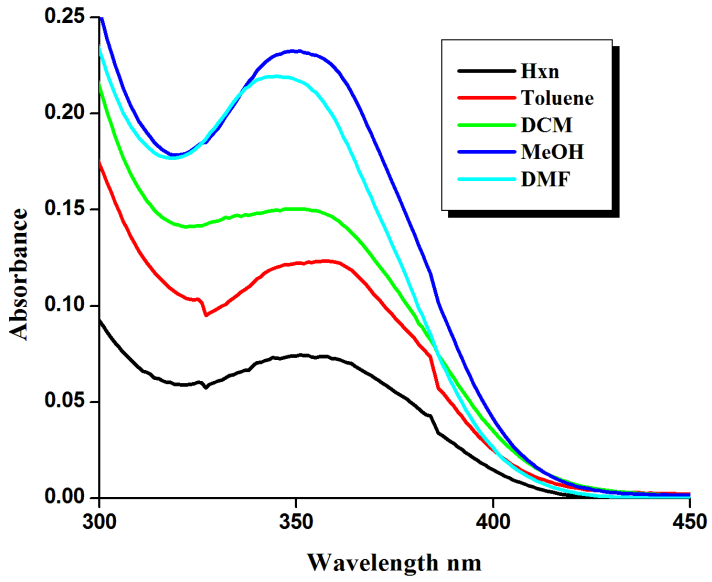

Fig. S7 The absorbance spectra of HL (1 x 10^{-5} M) in different solvents at room temperature.

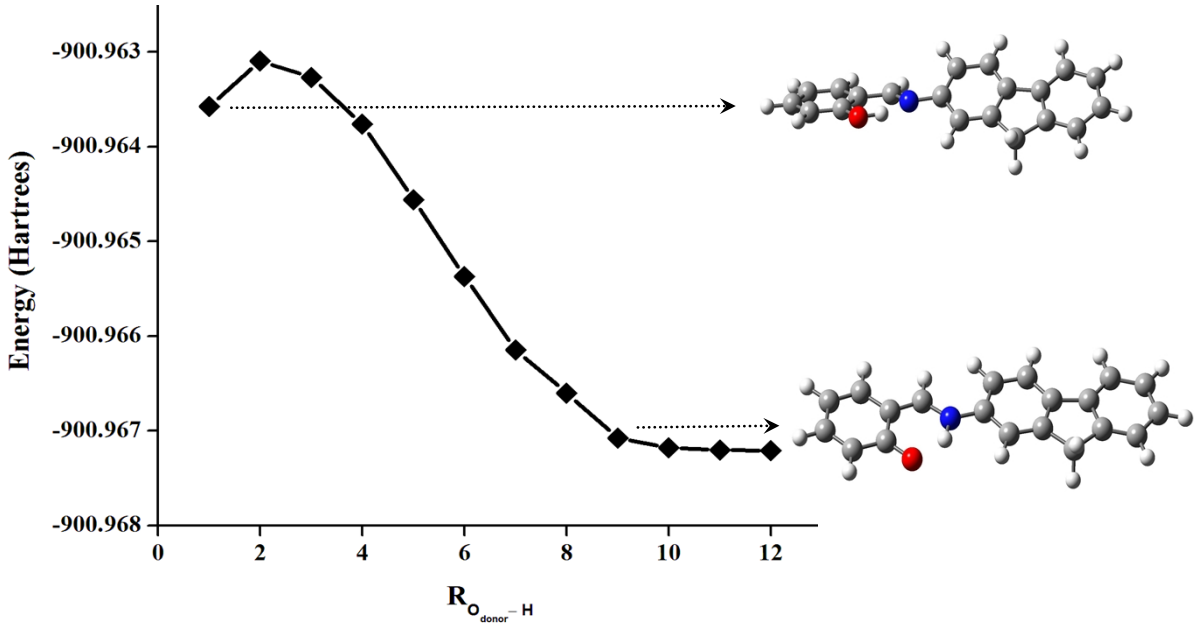

Fig. S8 potential energy curves for HL calculated at DFT/B3LYP level.

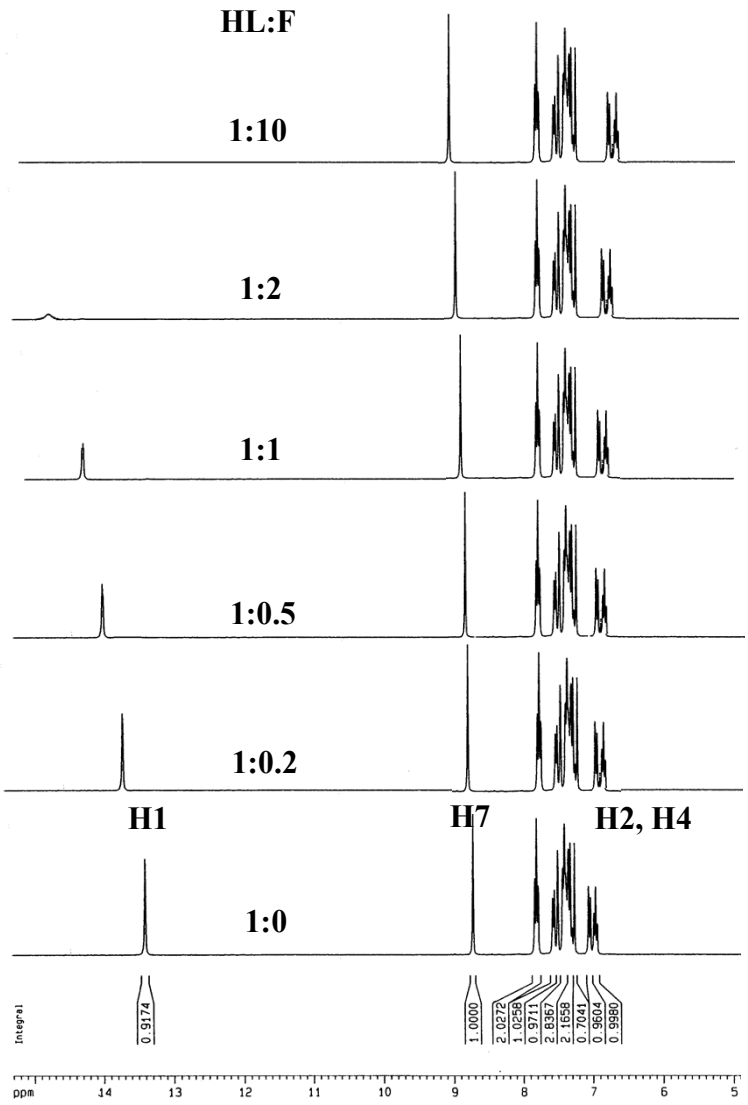

Fig. S9 ^{1}H NMR titration of HL with different concentration of F^{-} at room temperature.

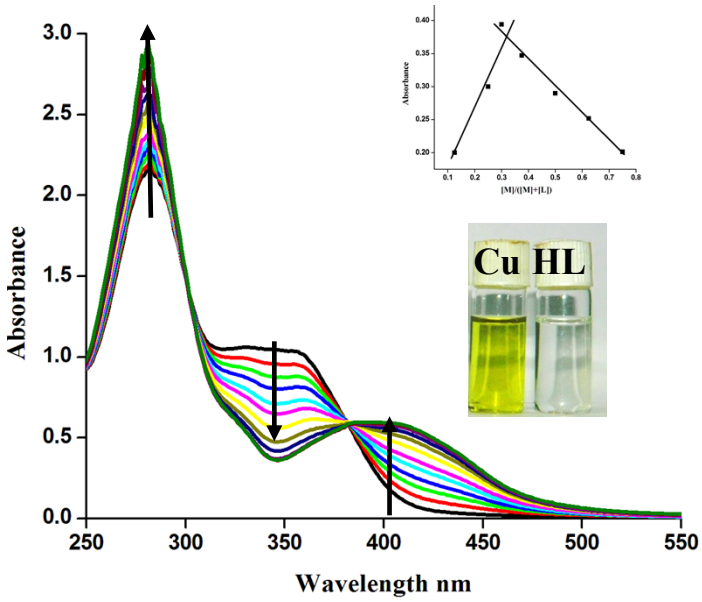

Fig. S10 Photographs of chemosensor HL in aqueous buffer–CH_3OH (2 : 1, v/v) at pH 7.2 in the presence of different cation under visible light; Spectrophotometric titrations of HL (10 μM) with various numbers of equivalent of Cu^{2+} at room temperature ([Cu^{2+}] = (0–7 x 10^{-6} M). Insets: the corresponding titration profiles confirm the 2:1 (HL: Cu^{2+}) binding stoichiometry.

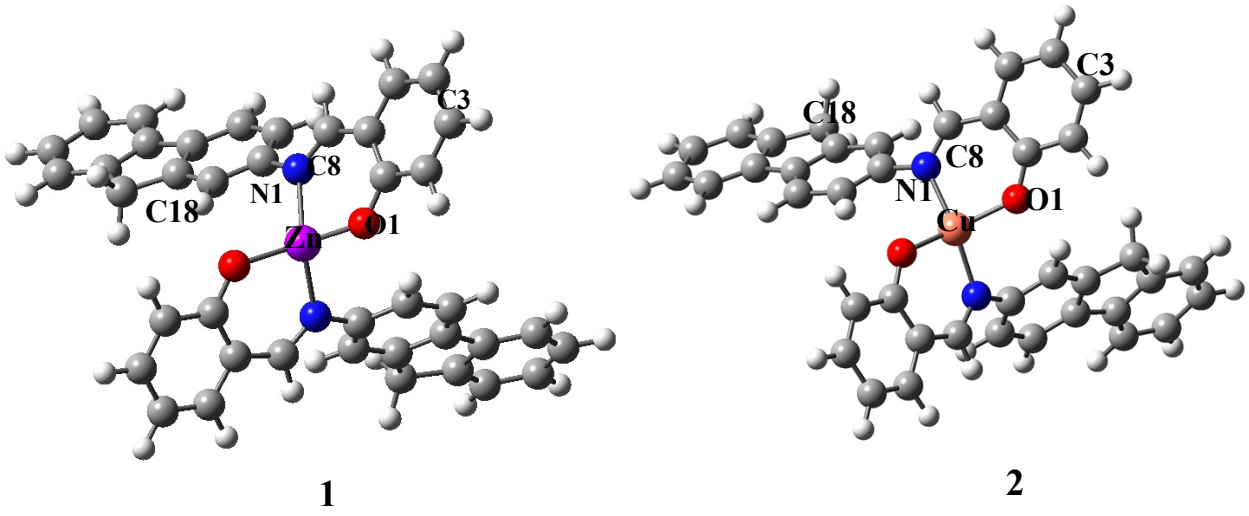

Fig. S11 Optimized molecular structures of **1** and **2**. (Zn: Violet, Cu: Orange, N: Blue, N and C: Grey. Hydrogen atoms are omitted for clarity).

Table S1 Frontier Molecular Orbital Composition (%) in the Ground State for complexes

	Orbital	Energy (eV)	Contribution (%) M	IM	FL	Ar	Main bond type
1	LUMO + 2	–1.05	1	4	89	6	π^* (FL)
	LUMO + 1	–2.09	0	42	21	37	π^*(FL)+π^*(IM)+ π^*(Ar)
	LUMO	–2.15	0	43	20	37	π^*(FL)+π^*(IM)+ π^*(Ar)
	HOMO	–5.76	1	7	31	61	π (FL)+ π (Ar)
	HOMO – 1	–5.79	1	9	33	57	π (FL)+ π (Ar)
	HOMO – 2	–6.2	1	4	54	41	π (FL) + π (Ar)
2	LUMO + 2	–1.09	32	1	60	7	M(e_g) + π^*(FL)
	LUMO + 1	–2.14	10	45	17	28	M(d)+π^*(FL)+π^*(IM)+π^*(Ar)
	LUMO	–2.17	1	46	16	37	π^*(FL)+π^*(IM)+π^*(Ar)
	HOMO	–5.84	2	10	35	53	π(FL)+π(IM)+π(Ar)
	HOMO – 1	–5.91	9	9	50	30	π (FL)+ π (Ar)
	HOMO – 2	–6.24	12	4	42	43	M(d_{xy})+π (FL)+ π (Ar)

1	^{1}ILCT	Hole	Electron
405 nm	S_1 w = 0. 69 3.0984eV $\pi(L) \rightarrow \pi^*(L)$ λ_{exp} = 400 nm	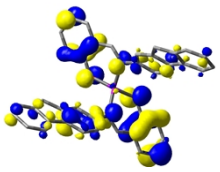	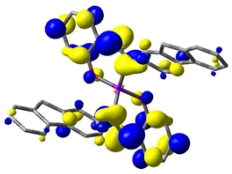
	S_2 w = 0. 63 3.1205eV $\pi(L) \rightarrow \pi^*(L)$ λ_{exp} = 397 nm	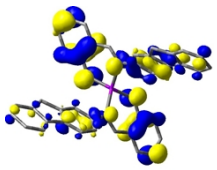	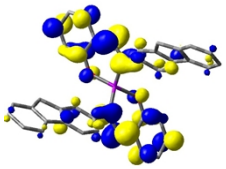
273 nm	S_{21} w = 0. 31 4.5541eV $\pi(L) \rightarrow \pi^*(L)$ λ_{exp} = 272 nm	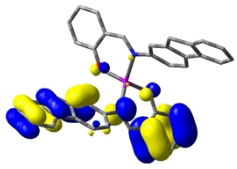	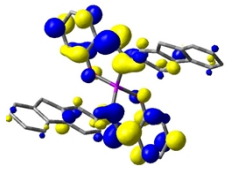
2	**^{1}MLCT / ^{1}ILCT**	**Hole**	**Electron**
413 nm	S_2 w = 0. 68 3.0107eV $t_{2g}+ \pi(L) \rightarrow \pi^*(L)$ λ_{exp} = 411 nm	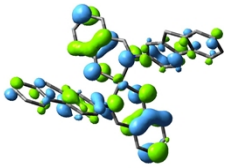	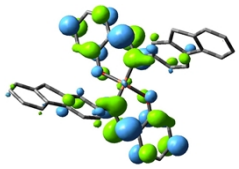
	S_3 w = 0.67 3.0232eV $\pi(L) \rightarrow \pi^*(L)$ λ_{exp} = 410 nm	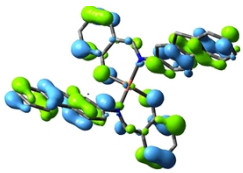	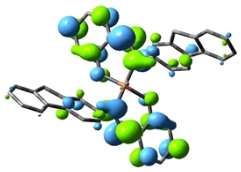
275 nm	S_{18} w = 0.59 4.4161 eV $\pi(L) \rightarrow \pi^*(L)$ λ_{exp} = 280 nm	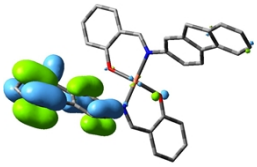	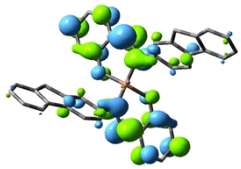
	S_{19} w = 0.47 4.4558 eV $e_g+ \pi(L) \rightarrow \pi^*(L)$ λ_{exp} = 278 nm	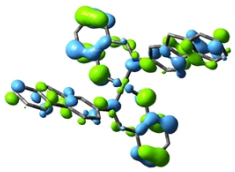	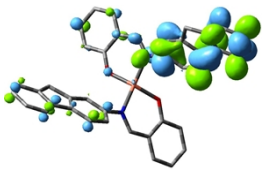

Fig. S12 Natural transition orbitals (NTOs) for the complexes **1** and **2** illustrating the nature of optically active singlet excited states in the absorption bands ~405 and 270 nm in methanol as a solvent.